QUANTITATIVE FINANCE
RESEARCH CENTRE

UNIVERSITY OF
TECHNOLOGY SYDNEY

QUANTITATIVE FINANCE RESEARCH CENTRE

Research Paper 398 This Version: March 2020

Dynamics of a Well-Diversified Equity Index

Eckhard Platen and Renata Rendek

ISSN 1441-8010 www.qfrc.uts.edu.au

Dynamics of a Well-Diversified Equity Index

March 30, 2020

Eckhard Platen[⋆] [1,2,3] and **Renata Rendek** [4]

Abstract: The paper derives a parsimonious model for the long-term dynamics of a well-diversified stock index, the S&P500. The total return index is modeled as growth optimal portfolio. Its real value evolves as the product of an exponential function of time and an ergodic diffusion, the normalized index. The latter evolves in some market time and is the inverse of the squared volatility which satisfies a novel volatility drift condition. Among the respective ergodic diffusions considered, only the derived square root process of dimension four provides dynamics that match stylized empirical facts. The derivative of market time turns out to be well approximated by a linear function of the squared derivative of a moving average of a proxy of the single driving Brownian motion. The resulting model volatility appears to be rough when viewed in calendar time. It explains well the dynamics of S&P500 data and allows the extraction of the paths of the model volatility and the Brownian motion. The proposed model is highly tractable.

Key words and phrases: long-term index model, volatility drift condition, rough volatility, leverage effect puzzle, benchmark approach, growth optimal portfolio.

JEL Classification: G10, C10, C15

1991 *Mathematics Subject Classification:* 62P05, 62P20, 62G05, 62-07, 68U20

Supported by Australian Research Council Grant: DP130104074

[1]University of Technology Sydney, School of Mathematical and Physical Sciences and Finance Discipline Group, PO Box 123, Broadway, NSW, 2007, Australia,
Email: Eckhard.platen@uts.edu.au, Phone: +61295147759.

[2]College of Business and Economics, Australian National University, Canberra.

[3]University of Cape Town, Department of Actuarial Science.

[4]University of Technology Sydney, Quantitative Finance Research Centre, School of Mathematical and Physical Sciences.

1 Introduction

The accurate modeling and theoretical understanding of the long-term dynamics of a well-diversified equity index, e.g. the S&P500, have been challenging tasks. No agreement has so far emerged in the literature what a reasonably accurate, long-term index model should look like. The stock market index appears to evolve in its own market time, as pointed out in Clark (1973): 'On days when no new information is available, trading is slow, and the price process evolves slowly. On days when new information violates old expectations, trading is brisk, and the price process evolves much faster'. New information is typically causing index moves and the challenge is to capture the feedback to such moves in a parsimonious model that explains the observed index dynamics and with it the model volatility.

The traditional focus on modeling volatility as a separate stochastic process seems to have hindered an early solution of this modeling challenge. It encounters the difficulty that the model volatility is somehow hidden and only observed indirectly through the estimated volatility. Moreover, when using estimated volatility for a given observation frequency as input, it is extremely difficult to infer the dependence between the hidden model volatility and the index. In Ait-Sahalia, Fan & Li (2013) these modeling difficulties have been labeled as the *leverage effect puzzle*. Moreover, volatility estimated from high-frequency data revealed that volatility paths are rough with many spikes; see e.g. Bayer, Friz & Gatheral (2016) and Gatheral, Thibault & Rosenbaum (2018). The estimated rough volatility requests accurate parsimonious modeling based on a proper understanding of the index dynamics.

'Ad hoc' models, typically chosen for tractability, dominate the literature. Adding another 'ad hoc' model to reflect, for instance, the observed roughness of volatility would not provide much progress in the understanding of the dynamics of well-diversified stock indexes. We aim to change this unsatisfactory situation by *deriving* a new class of models based on three crucial properties that stock indexes can be expected to have. These properties involve the notion of a *growth optimal portfolio* (GP), which is the portfolio maximizing expected logarithmic utility; see Kelly (1956) and Merton (1992). Furthermore, they exploit for the first time in the literature some similarity between well-diversified wealth dynamics and population size dynamics of birth-and-death-processes, also known as branching processes; see Feller (1971). We list below the three properties which turn out to hold the key to the understanding of well-diversified index dynamics:

- A well-diversified total return stock index is a proxy of the respective growth optimal portfolio.
- In some market time the index evolves similarly to the continuous time limit

of the population size of a birth-and-death process.

- The derivative of the market time is a function of the derivative of a moving average of a proxy of the single driving Brownian motion.

The first two properties determine the 'normal' dynamics of the index, which concerns its evolution in some market time. The third property characterizes the market time, which accelerates the 'normal' index dynamics when the Brownian motion, and thus the index, moves further away from its recent levels. The third property leaves deliberately some freedom for the specification of the function determining the derivative of market time, the market activity, which can be expected to vary slightly for different markets and over time.
From the above three properties we derive a new class of parsimonious models, which is nested in continuous time finance, pioneered by Merton (1973). The models of this class are highly tractable. Noteably, they lead beyond classical finance assumptions and are, therefore, derived under the benchmark approach; see Platen (2002) and Platen & Heath (2010).

To be directly applicable and comparable with other index models, the current paper focuses on modeling the long-term dynamics of the real value, total return S&P500. We use an in early years in Shiller (2015) constructed version of the S&P500, which is arguably the best studied stock index and appears to have the above mentioned three properties. The paper discovers the fact that the market activity is for the S&P500 close to a linear function of the square of the derivative of a moving average of a proxy of the driving Brownian motion. This crucial fact allows us to fit well the derived model to monthly observed S&P500 data. It permits also the extraction of the paths of hidden model components, in particular, those of the market activity, the model volatility and the single driving Brownian motion.
A challenge represents the control of the impact of numerical errors in the extraction of hidden model components when using monthly observed data. Employing higher-order, implicit Wagner-Platen expansions, see Chapter 4 in Platen & Bruti-Liberati (2010) and Chapter 5 in Kloeden & Platen (1999), for approximating increments of components of the solution of the model's stochastic differential equation (SDE) is shown to numerically stabilize the extraction of hidden paths.

The proposed inference of the model parameters and extraction of the hidden Brownian motion path 'inverts' the well-known scenario simulation for an SDE, e.g. described in Chapter 12 in Kloeden & Platen (1999), where the Brownian motion is the input. In the current paper the model postulates a potential Brownian motion path, which becomes the output and is extracted using stochastic expansions of increments of observed components. It is then a question whether the extracted path cannot be rejected as that of a true Brownian motion.
The proposed new model class generates naturally the well-known leverage ef-

fect; see e.g. Black (1976). It also predicts and explains the general roughness of volatility, which so far has been observed for volatility paths estimated from high-frequency data but becomes now also apparent for monthly data.

Additionally to the derivation of the proposed model class, the paper studies the appropriateness of other popular volatility model classes for capturing the long-term dynamics of a stock index when interpreted as GP. This leads to the discovery of a novel *volatility drift condition*, which the considered volatilities have to satisfy.

As shown in Platen & Rendek (2008), the log-return distribution of well-diversified stock indexes is with high significance close to that of a Student-t distribution with four degrees of freedom. Among the volatility model classes considered in this paper only the derived model class matches this property together with other empirical stylized properties of stock indexes.

The paper is organized as follows: Section 2 describes, illustrates and fits the derived model to the S&P500. Section 3 briefly reviews the literature on volatility and index modeling from the perspective of the proposed model. Section 4 derives the proposed model by assuming the earlier mentioned three properties. Finally, several popular volatility model classes applied to GP dynamics are discussed in Section 5.

2 Long-Term Index Model

2.1 Model

In this section we present the proposed model, where we defer the discussion of its links to the literature to Section 3 and its derivation to Section 4. The real (in units of the consumer price index denominated) value S_{τ_t} at calendar time t of a well-diversified total return (dividends reinvested) stock index is modeled by the product

$$S_{\tau_t} = A_{\tau_t} Y_{\tau_t}, \tag{2.1}$$

for $t \geq 0$. The normalized index Y_{τ_t} follows in some market time $\tau = \{\tau_t, t \geq 0\}$ a square root process of dimension four, see Revuz & Yor (1999), with SDE

$$dY_{\tau_t} = (1 - Y_{\tau_t})d\tau_t + \sqrt{Y_{\tau_t}} dW_{\tau_t}, \tag{2.2}$$

for $t \geq 0$ with $Y_0 = \frac{S_0}{A_0} > 0$. Here $W = \{W_\tau, \tau \geq 0\}$ is the single driving Brownian motion that models the uncertainty of the index dynamics in some market time τ. The normalization A_{τ_t} is defined at time t as

$$A_{\tau_t} = A \exp(\tau_t + lt), \tag{2.3}$$

where we call l the excess growth rate and $A > 0$ the normalization parameter.

The market time

$$\tau_t = \int_0^t M_s ds \tag{2.4}$$

at calendar time $t \geq 0$ equals the integrated market activity. The market activity

$$M_t = \xi \left(U_t^{'} \right)^2 + \varepsilon \tag{2.5}$$

is modeled as a linear function of the square of the derivative

$$U_t^{'} = \frac{dU_t}{dt} = \lambda(2Y_{\tau_t}^{1/2} - U_t) \tag{2.6}$$

with $U_0 = 2Y_{\tau_0}^{1/2}$ of the (by (2.6) determined) moving average U_t of twice the square root of the normalized index Y_{τ_t}.

The three state variables of the above proposed model are the normalized index Y_{τ_t}, the normalization A_{τ_t} and the moving average U_t. The normalization parameter A brings the normalized index dynamics to its standard level, as we will see later on. The moving average U_t can be interpreted by (2.6) and later on by (2.24) locally as a smoothed proxy for the single driving Brownian motion W. The three parameters characterizing the market activity, consist of the base activity $\varepsilon > 0$, the activity scale $\xi > 0$ and the speed of adjustment $\lambda \geq 0$. These parameters are all economically meaningful, as becomes clear when deriving the model in Section 4.

Setting the market activity $M_t = m > 0$ constant, yields an in calendar time linear market time $\tau_t = mt$ for a stylized version of the proposed model. By modifying the function (2.5) to model varying properties of market activity one obtains other models, which we interpret as models from the new in the current paper proposed model class.

2.2 Fitting the Model in Market Time

By employing monthly observed real value S&P500 total return index data, we illustrate in the following key features of the above proposed model. The monthly data from January 1871 until February 2020 we use is for the early years constructed analogously to the S&P500 and taken from Shiller's web site; see Shiller (2015). To fix the in units of the consumer price index denominated S&P500 total return price index S_{τ_t}, $t \geq 0$, we scale the index such that it starts at the beginning of January 1871 with the value $S_{\tau_0} = 1.0$. This scaling does not create any loss of generality because starting with another initial value would simply change the normalization parameter A accordingly.

We fit in this subsection the model in market time by estimating the excess growth rate l and the normalization parameter A. Both have to be interpreted as drift parameters, which are notoriously difficult to estimate. The available observation windows for estimating parameters in drift coefficients of SDEs for financial securities are often too short to provide useful estimates; see e.g. DeMiguel, Garlappi & Uppal (2009). However we will see, the above long-term model can be meaningfully fitted to the S&P500 by using an observation window of at least 70 years, which is rather long but not as long as what Black-Scholes type models would require. This practically important property emerges because the normalized index appears to be realistically modeled by an ergodic process, which makes the estimation of the excess growth rate possible.
One may ask, why do we model the dynamics of the real value of the total return index? The reason is that real prices can be expected to revert in the long-term to respective hidden underlying fundamental values, which can be assumed to be reasonably stable. Interest rates, inflation rates and currencies can be influenced by the Souvereign to control the respective economy. Studying price evolutions in currency or savings account denomination can significantly distort over long periods of time the natural reversion of a price process to its underlying hidden fundamental value. In some sense, the normalization A_{τ_t} can be interpreted as a proxy for the fundamental value of the index. In the absence of information beyond the one provided by the real total return index price, where its logarithm appears to mean-revert around a straight line (see Figure 2.2), setting the hidden excess growth rate to a constant appears to be a reasonable approximation.

2.2.1 Estimating the Excess Growth Rate

For convenience, we introduce the standardized index value

$$\tilde{S}_{\tau_t} = \frac{S_{\tau_t}}{A \exp(lt)} = Y_{\tau_t} \exp(\tau_t). \tag{2.7}$$

Its logarithm satisfies by (2.2) and the Itô formula the SDE

$$d \ln(\tilde{S}_{\tau_t}) = \frac{1}{2} \frac{\exp(\tau_t)}{\tilde{S}_{\tau_t}} d\tau_t + \sqrt{\frac{\exp(\tau_t)}{\tilde{S}_{\tau_t}}} dW_{\tau_t}. \tag{2.8}$$

We notice that the integrated expected growth rate of the logarithm of the standardized index equals half its quadratic variation. Furthermore, this quadratic variation equals that of the logarithm of the index. This means, the average drift $\bar{m}(t)$ of the logarithm of the standardized index can be estimated via the formula

$$\bar{m}(t) = \frac{0.5}{t} [\ln(S_{\tau_\cdot})]_t \tag{2.9}$$

for $t > 0$. Here $[X_\cdot]_t$ denotes the quadratic variation of a process $X = \{X_t, t \geq 0\}$, which is approximated by the sum of the squares of the increments of X when

the time step size converges to zero.
As indicated above, the logarithm of the standardized index $\ln(\tilde{S}_{\tau_t})$ and half the quadratic variation of the logarithm of the index evolve similarly in the long-term. Hence, the excess growth rate l can be estimated as the extra average growth rate that the index achieves beyond that of its standardized dynamics. Therefore, over a sufficiently long observation window the excess growth rate l is approximated by the time average of the growth rate of the index minus the time average of the growth rate of the standardized index $\bar{m}(t)$. Thus, for a sufficiently long observation window $[0, t]$ the excess growth rate of the index can be captured approximately via the formula

$$\hat{l}(t) = \frac{1}{t} \ln(S_t/S_0) - \bar{m}(t). \tag{2.10}$$

Note that this estimate does only require the observation of the logarithm of the index and its quadratic variation. We emphasize that a particular volatility dynamic is here not exploited or assumed. Thus, for all volatility model classes we consider later on in Section 5, the above estimator for the excess growth rate can be applied. We show in Figure 2.1 the estimate $\hat{l}(t)$ in dependence on t and notice that it stabilizes after 70 years of observation. By using the entire available observation window we obtain for the assumed constant l the estimate $\hat{l}(149) \approx 0.057$.

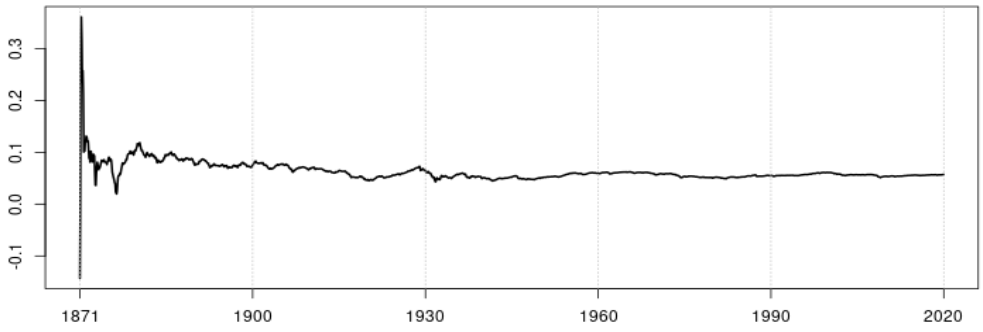

Figure 2.1: Excess growth rate estimate $\hat{l}(t)$ in dependence on time t.

2.2.2 Estimating the Normalization Parameter

By application of the Itô formula to (2.8) we obtain for $\sqrt{\tilde{S}_{\tau_t}}$ the SDE

$$d\sqrt{\tilde{S}_{\tau_t}} = \frac{3}{8} \frac{\exp(\tau_t)}{\sqrt{\tilde{S}_{\tau_t}}} d\tau_t + \frac{1}{2} \sqrt{\exp(\tau_t)} dW_{\tau_t}. \tag{2.11}$$

The market time τ_t satisfies for $t > 0$ the formula

$$\tau_t = \ln\left(4[\sqrt{\tilde{S}_\cdot}]_{\tau_t} + 1\right). \tag{2.12}$$

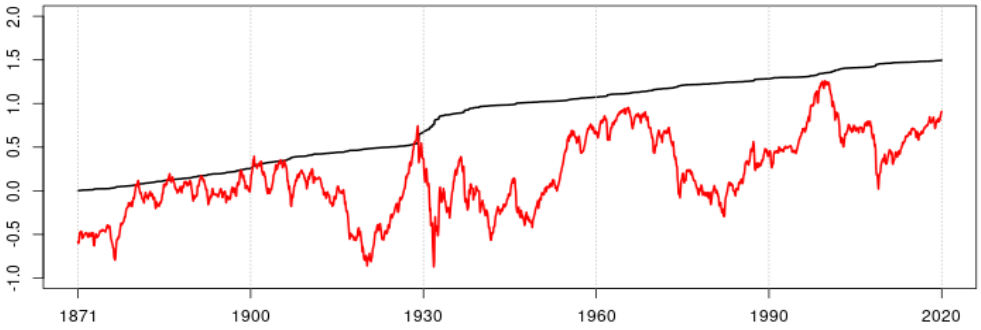

Figure 2.2: Logarithm $ln(\tilde{S}_{\tau_t})$ of the standardized index and estimated market time $\hat{\tau}_t$.

We can approximate the quadratic variation on the right hand side of (2.12) by the sum

$$[\sqrt{\tilde{S}_\cdot}]_{\tau_{t_i}} \approx \sum_{k=1}^{i} \left(\sqrt{\tilde{S}_{\tau_{tk}}} - \sqrt{\tilde{S}_{\tau_{tk-1}}}\right)^2 \tag{2.13}$$

for $i = 1, 2, \ldots, N$. N is here the number of observations and $0 = t_0 < t_1 < \cdots < t_i < \cdots < t_N$ are the observation times. For the monthly observations of the S&P500 we set $t_i = t_{i-1} + \frac{1}{12}$. The estimated market time $\hat{\tau}_{t_i}$ at the calendar time t_i is then by (2.12) and (2.13) obtained via the formula

$$\hat{\tau}_{t_i} = \ln\left(4\sum_{k=1}^{i} \left(\sqrt{\tilde{S}_{\tau_{tk}}} - \sqrt{\tilde{S}_{\tau_{tk-1}}}\right)^2 + 1\right). \tag{2.14}$$

We display in Figure 2.2 the logarithm $\ln(\tilde{S}_{\tau_t})$ of the standardized index together with the estimated market time $\hat{\tau}_t$. We emphasize that Figure 2.2 confirms visually the remarkable theoretical fact that due to (2.7) we have $\ln(\tilde{S}_{\tau_t}) = \ln(Y_{\tau_t}) + \tau_t$, which means that the logarithm of the standardized index increases under the derived model in the long-term, on average, analogous to the market time.

The average slope

$$\hat{m}(t) = \frac{1}{t}\hat{\tau}_t \tag{2.15}$$

of the market time can, thus, be interpreted for large enough t as an estimate for the average market activity. By equating $\hat{m}(t)$ and $\bar{m}(t)$ using the estimators (2.15) and (2.9), respectively, one can solve for a given observation window $[0, t]$ the resulting equation to obtain for the normalization parameter A the estimator

$$\hat{A}(t) = \frac{4\left[\sqrt{\frac{S_{\tau_\cdot}}{\exp(l_\cdot)}}\right]_t}{\exp(0.5[\ln(S_{\tau_\cdot})]_t) - 1}, \tag{2.16}$$

where its value is shown in Figure 2.3 as it evolves over time. Also here we see that the estimate stabilizes after about 70 years. By using the entire available

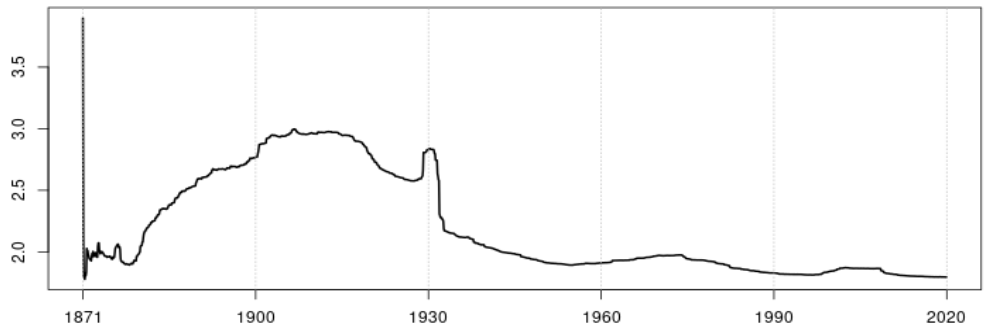

Figure 2.3: Normalization parameter estimate $\hat{A}(t)$ in dependence on time t.

observation window we obtain the estimate $\hat{A}(149) \approx 1.8$.

With these estimated parameters we extract according to (2.14) the estimated market time $\hat{\tau}_t$, which we display in Figure 2.2. Finally, we calculate the average market activity $\hat{m}(149) \approx 0.01$ using (2.15) for the entire available observation window. This estimate together with $\hat{l}(149)$ and $\hat{A}(149)$ provides a fit for the stylized version of the model.

2.3 'Normal' Volatility

We have fitted the excess growth rate l and the normalization parameter A and estimated the market time shown in Figure 2.2. This allows us to observe the 'normal' volatility θ_{τ_t} as the volatility with respect to market time, given by (2.8) and (2.7) as

$$\theta_{\tau_t} = \left(\frac{A\exp(lt + \tau_t)}{S_{\tau_t}}\right)^{\frac{1}{2}} = \frac{1}{\sqrt{Y_{\tau_t}}}. \tag{2.17}$$

This is the 'normal' volatility of the normalized index but also the 'normal' volatility of the standardized index and the index itself.

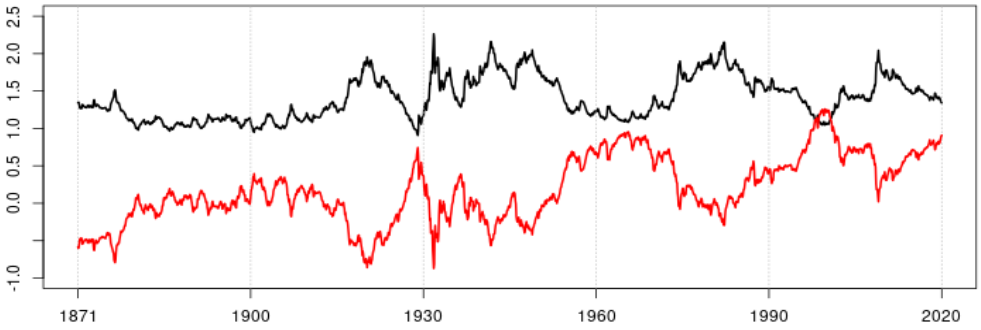

Figure 2.4: 'Normal' volatility θ_{τ_t} (black) and logarithm of standardized index $\ln(\tilde{S}_{\tau_t})$ (red) .

We include in Figure 2.4 not only the 'normal' volatility θ_{τ_t} (in black on top) but also the logarithm of the standardized index $\ln(\tilde{S}_{\tau_t})$ (in red). One observes that the 'normal' volatility increases when the index decreases and vice versa, which models naturally the well-known leverage effect, an extremely important stylized empirical fact; see Black (1976). More precisely, the squared 'normal' volatility $(\theta_{\tau_t})^2$ equals by (2.17) the inverse of the normalized index, which satisfies by (2.2) and application of the Itô formula the SDE

$$d\,(\theta_{\tau_t})^2 = (\theta_{\tau_t})^2\,d\tau_t - ((\theta_{\tau_t})^2)^{\frac{3}{2}} dW_{\tau_t}. \tag{2.18}$$

One notes in the diffusion coefficient of this SDE the power 3/2, which identifies the 'normal' volatility dynamics as those of a 3/2-volatility model. The 3/2-volatility model was originally proposed in Platen (1997) as an early step in the development of the benchmark approach. It was independently suggested in Heston (1997) because of its tractability as inverse of a square root process. Key features of a 3/2-volatility model are the rather high power of 3/2 in the diffusion coefficient of the SDE (2.18), which can reduce or increase rapidly the heteroscedasticity of volatility. Note that the above 3/2-volatility model is the volatility dynamics of the stylized version of the proposed model with constant market activity $M_t = m$.

The SDE (2.2) for the normalized index Y_{τ_t} is that of a square root process (CIR process) of dimension four in τ-time with reference level 1.0; see Revuz & Yor (1999). The mean-reversion rate or speed of adjustment parameter of the normalized index with respect to market time has in the SDE (2.2) the value 1.0, which indicates in market time a half-life time of $\ln(2) \approx 0.693$ for shocks to the normalized index. When taking into account the average market activity of about $\hat{m}(149) \approx 0.01$, this translates into a half-life time of about $\ln(2)/\hat{m}(149) \approx 70$

calendar years. This means that the normalized index evolves very slowly with a half-life time of shocks of more than the length of a working life. This hints at the fact that it may be unreasonable to expect meaningful estimates for the excess growth rate and the normalization parameter from data covering an observation window of less than 70 years.
Furthermore, the stationary density of the normalized index is that of a gamma density with four degrees of freedom; see Revuz & Yor (1999). Thus, when estimating the density of log-returns of the index, these log-returns would appear to generate a normal mixture density where the mixing random variance is that of the inverse of a gamma distributed random variable. This is yielding a Student-t density of four degrees of freedom as normal-mixture density for estimated log-returns; see e.g. Platen & Rendek (2008). Empirical evidence, e.g. in Markowitz & Usmen (1996a), Markowitz & Usmen (1996b), Hurst & Platen (1997), Fergusson & Platen (2006) and Platen & Rendek (2008), shows that well-diversified stock indexes have log-returns that with high significance cannot be rejected as being Student-t distributed with about four degrees of freedom. Thus, the proposed model generates the leptokurtic log-return distribution that is observed in reality.

2.4 Model Market Activity

To complete the model fit we need to model the dynamics of the market time τ_t, see (2.4), which requires estimating the speed of adjustment λ, the activity scale ξ and the base activity ε. The formula (2.5) for the market activity employs the moving average U_t, determined by the differential equation (2.6). For extracting the model market activity the increments of the solution of this differential equation can be approximated via Wagner-Platen expansions; see Platen & Bruti-Liberati (2010).
As pointed out in Chapter 12 of Kloeden & Platen (1999) and Chapter 14 of Platen & Bruti-Liberati (2010), substantial numerical errors may arise when employing for large time step sizes explicit Wagner-Platen expansions. For the rather large time step size of monthly observed S&P500 data this appears to be the case. To control these numerical errors, the semi-drift-implicit Wagner-Platen expansion

$$U_{t_i} \approx \left(U_{t_{i-1}} \left(1 - \frac{\lambda}{2} \Delta \right) + \lambda \Delta \left(Y_{\tau_{t_i}}^{\frac{1}{2}} + Y_{\tau_{t_{i-1}}}^{\frac{1}{2}} \right) \right) \left(1 + \frac{\lambda}{2} \Delta \right)^{-1} \tag{2.19}$$

for $\Delta = t_i - t_{i-1}$, $i \in \{1, 2, \ldots, N\}$, with $U_{t_0} = 2Y_{\tau_{t0}}^{\frac{1}{2}}$ is employed, suggested for scenario simulation in Section 12.2 of Kloeden & Platen (1999). Since the market activity can move extremely fast, such an implicit stochastic expansion was found to be necessary when using monthly observed S&P500 data.
In Figure 2.5 we display the trajectory of the quantity $2Y_{\tau_t}^{\frac{1}{2}}$ (black) together with

its moving average U_t (red). We notice visually almost no difference between both trajectories. Only when extreme index moves arise, the moving average lags slightly behind and does not reach the extreme values.

Figure 2.5: $2Y_{\tau_t}^{\frac{1}{2}}$ (black) and its moving average U_t (red).

Now, we can calculate according to (2.5) and (2.6) the model market activity

$$M_{t_i} = \xi\lambda^2(2Y_{\tau_{t_i}}^{1/2} - U_{t_i})^2 + \varepsilon \tag{2.20}$$

to form the approximate integrated model market activity

$$\tilde{\tau}_{t_i} \approx \sum_{k=1}^{i} M_{t_k}\Delta, \tag{2.21}$$

which we call model market time, where $\Delta = t_k - t_{k-1}$ for $k = 1, \ldots, N$, with N denoting the number of observations. We note from (2.20) that the market time accelerates significantly when the index moves substantially.

For estimating the parameters for the speed of adjustment λ, the activity scale ξ and the base activity ε, we form the least squares distance

$$\min_{\lambda,\xi,\varepsilon} \frac{1}{N} \sum_{i=1}^{N} (\tilde{\tau}_{t_i} - \hat{\tau}_{t_i})^2 \tag{2.22}$$

between the above model market time $\tilde{\tau}_{t_i}$ and the previously extracted estimated market time $\hat{\tau}_{t_i}$; see (2.12). We obtain for monthly observed data the least squares parameter estimates $\hat{\lambda} = 8.1$, $\hat{\xi} = 0.14$ and $\hat{\varepsilon} = 0.0028$, respectively.
The resulting model market activity M_t is exhibited in Figure 2.6. It can be seen from formula (2.5) that it is the square of the derivative U_t' which causes the clearly visible spikes in the market activity shown in Figure 2.6. These spikes

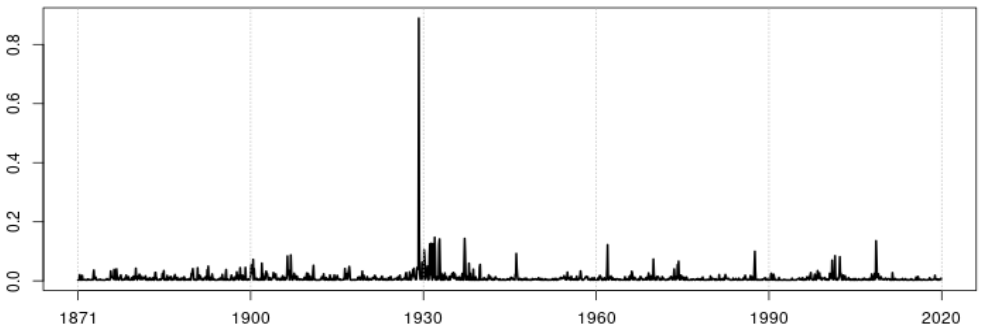

Figure 2.6: Model market activity M_t.

and the obvious roughness of the market activity M_t are consequences of the fact that U_t' is the derivative of U_t, which is smoothing the *non-differentiable* path of $2Y_{\tau_t}^{\frac{1}{2}}$. As we will see later on in (2.24), the fluctuations of this non-differentiable path are those of the driving Brownian motion. Only the drift in the SDE for $2Y_{\tau_t}^{\frac{1}{2}}$ deviates from zero and $2Y^{\frac{1}{2}}$ is in τ-time an ergodic process, whereas W is in τ-time a martingale. Note that over shorter time periods the paths of $2Y^{\frac{1}{2}}$ and W look almost identical. However, over longer periods the mean-reversion of $2Y^{\frac{1}{2}}$ pulls this process back to a long-term average level. On the other hand, the best forecast for future values of W is always its current value.

We note in Figure 2.6 that the market activity becomes sometimes rather high when it spikes, e.g. at the dramatic drawdown during the Great Depression after August 1929. Consequently, for the logarithm of the standardized index in Figure 2.2 this drawdown occurs extremely fast, a feature that is difficult to capture with a scalar diffusion. Figure 2.7 shows the model market time $\tilde{\tau}_t$ (black) together with the estimated market time $\hat{\tau}_t$ (red). The estimated market time $\hat{\tau}_t$ uses the observed approximate quadratic variation in (2.13), whereas $\tilde{\tau}_t$ is calculated according to the derived model equations. We note a good fit of both trajectories over the entire 149 year period.
It is clear that the activity scale can be expected to change slightly over time due to changes in general trading activity triggered, e.g., by extreme drawdowns. Indeed, the slight differences between both trajectories in Figure 2.7 almost vanish when allowing the activity scale to switch in September 1929 and in June 1942. More precisely, the activity scale during the Great Depression seems to have moved slightly up from about $\hat{\xi} \approx 0.14$ to a level of about $\hat{\xi} \approx 0.16$ and seems to have fallen after June 1942 to a level of about $\hat{\xi} \approx 0.11$. Thus, one can improve models in the proposed model class by making the activity scale (and if necessary other parameters) time dependent. This opens an interesting area of research for modeling the dynamics of stock indexes, which is of particular importance for data

observed with higher frequencies. Forthcoming work will study more frequently observed stock index data, where it turns out that the above estimated parameters provide already a good fit for daily observed S&P500 data, which then can be improved by making the activity scale change after major extreme drawdowns.

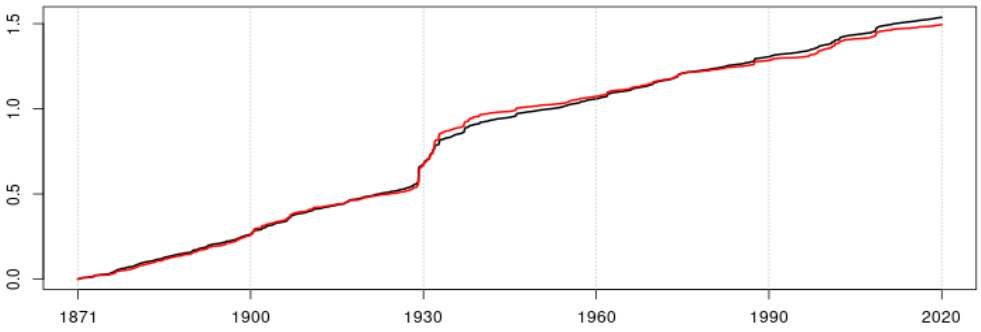

Figure 2.7: Approximate integrated model market activity $\tilde{\tau}_t$ (black) and estimated market time $\hat{\tau}_t$ (red).

2.5 Model Volatility

According to (2.8) and (2.4) we calculate the model volatility via the formula

$$\sigma_t = \sqrt{M_t}\theta_t \tag{2.23}$$

and display σ_t for the S&P500 in Figure 2.8. The path of the usually hidden model volatility has spikes. Its visible roughness is explained through the roughness of the model market activity shown in Figure 2.6. Thus, the proposed model offers a natural explanation for the in recent years intensily investigated phenomenon of rough volatility, see e.g. Bayer, Friz & Gatheral (2016) and Gatheral, Thibault & Rosenbaum (2018), which became visible when estimated volatility was obtained from high-frequency data. We emphasize that the model volatility extracted from monthly data exhibits already the typical roughness of volatility and one has not to use high-frequency data to observe the roughness of volatility. Moreover, it becomes clear that it is the roughness of the market activity, which is obviously linked to that of trading activity, that causes the roughness of volatility.

In the earlier literature one focuses typically on modeling the estimated volatility $\hat{\sigma}_t$, which we obtain in this paper by standard volatility estimation, that is, via exponential smoothing of squared observed index log-returns, see e.g. RiskMetrics (1996), with decay parameter 0.94. When estimating $\hat{\sigma}_t$, the randomness of

squared log-returns and the delay effect caused by exponential smoothing create major differences between the estimated volatility $\hat{\sigma}_t$ and the with the fitted parameters calculated model volatility σ_t, which we both display in Figure 2.8. Visually one notes that whenever the model volatility (shown in black) spikes, the estimated volatility (shown in red) jumps up and declines slowly afterwards until the next major spike occurs. In this sense the estimated volatility is similar to some by a moving average smoothed model volatility, which is explained by the way the estimated volatility is calculated.
The correlation between the estimated volatility and the normalized index is quite different to the one between the 'normal' volatility and the normalized index. The latter two processes are by (2.18) and (2.2) perfectly negatively correlated, which models the leverage effect, whereas the other correlation is strongly influenced by the exponential smoothing that generates the estimated volatility. Through the proposed class of models the earlier mentioned leverage effect puzzle, pointed out in Ait-Sahalia, Fan & Li (2013), becomes explained.
Instead of comparing the trajectories of estimated volatility and model volatility it seems better to compare those of the integrated squared volatility, which equals the quadratic variation of the logarithm of the index, and the integrated squared model volatility. The respective trajectories turn out to be close to each other, similar to those of the estimated market time $\hat{\tau}_t$ and the integrated model market activity $\tilde{\tau}_t$, shown in Figure 2.7.

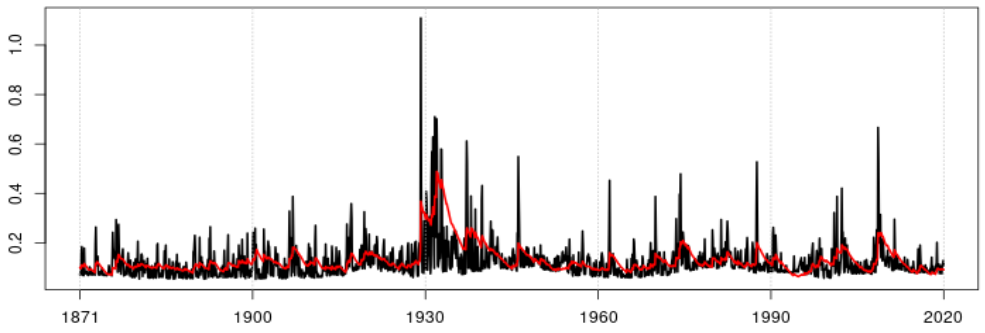

Figure 2.8: Model volatility σ_t (black) and estimated volatility $\hat{\sigma}_t$ (red)

2.6 Extracting the Postulated Brownian Motion Path

The following explicit formula for the Brownian motion value

$$W_{\tau_t} = 2\left(Y_{\tau_t}^{\frac{1}{2}} - Y_0^{\frac{1}{2}}\right) - \int_0^{\tau_t} \left(\frac{3}{4} Y_\tau^{-\frac{1}{2}} - Y_\tau^{\frac{1}{2}}\right) d\tau \tag{2.24}$$

follows from the SDE (2.2) via an application of the Itô formula. The equations (2.24) and (2.4) allow us to extract the increments of the by the model postulated Brownian motion W by approximating numerically the integral on the right-hand side of (2.24) using a drift-implicit Wagner-Platen expansion yielding

$$W_{\tau_{t_i}} - W_{\tau_{t_{i-1}}} \approx 2\left(Y_{\tau_{ti}}^{\frac{1}{2}} - Y_{\tau_{ti-1}}^{\frac{1}{2}}\right) - \left(\frac{3}{4}Y_{\tau_{ti}}^{-\frac{1}{2}} - Y_{\tau_{ti}}^{\frac{1}{2}}\right) M_{t_i}(t_i - t_{i-1}). \tag{2.25}$$

We show in Figure 2.9 the resulting estimated path of the postulated Brownian

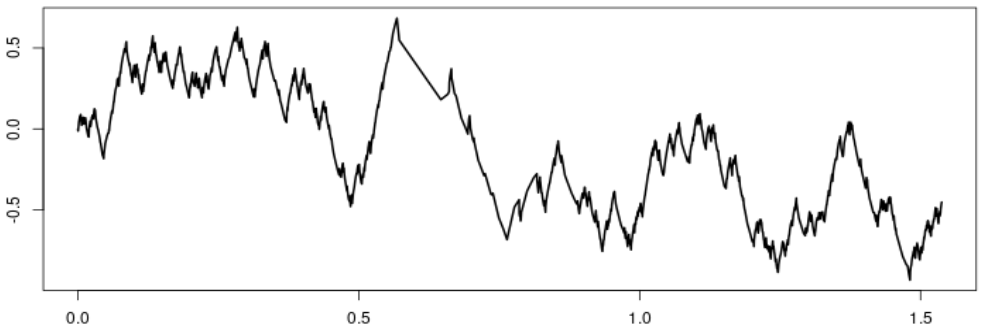

Figure 2.9: Estimated postulated Brownian motion path W in model market time $\tilde{\tau}$.

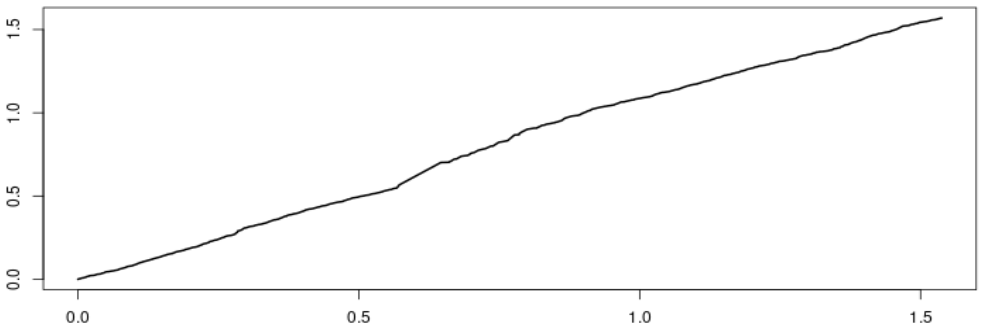

Figure 2.10: Quadratic variation $[W.]_{\tilde{\tau}}$ in model market time $\tilde{\tau}$.

motion W_τ in with fitted parameters calculated model market time $\tilde{\tau}$. Note that there are periods in market time where we have only a few observations, e.g. near $\tilde{\tau} \approx 0.6$, because the market activity is extremely high at that time during the Great Depression. To check whether the path in Figure 2.9 is possibly that of

a Brownian motion with respect to $\tilde{\tau}$-time, we plot in Figure 2.10 its quadratic variation $[W.]_{\tilde{\tau}}$ in $\tilde{\tau}$-time. It appears to be almost a straight line with average slope of about 1.0. Only close to $\tilde{\tau} \approx 0.6$ the graph curves up during the Great Depression and is then followed by a period with slightly lower than theoretically predicted slope until the end of the observation period. Most of these deviations from a straight line with slope 1.0 are a consequence of the assumed constant activity scale. When making the parameter ξ time dependent in the way as indicated at the end of Subsection 2.4, then the quadratic variation $[W.]_{\tilde{\tau}}$ in $\tilde{\tau}$-time becomes visually almost indistinguishable from a straight line with slope 1.0.

Given the increments of the postulated Brownian motion with respect to market time, W, we can extract its standardized increments $\tilde{W}_{t_i} - \tilde{W}_{t_{i-1}}$ via the approximate formula

$$\tilde{W}_{t_i} - \tilde{W}_{t_{i-1}} \approx 0.5\left(\frac{1}{\sqrt{M_{t_i}/12}} + \frac{1}{\sqrt{M_{t_{i-1}}/12}}\right)\left(W_{\tau_{t_i}} - W_{\tau_{t_{i-1}}}\right), \tag{2.26}$$

which reduces the impact of numerical errors by standardizing with a symmetric average for each observation interval. We display in Figure 2.11 the autocorrela-

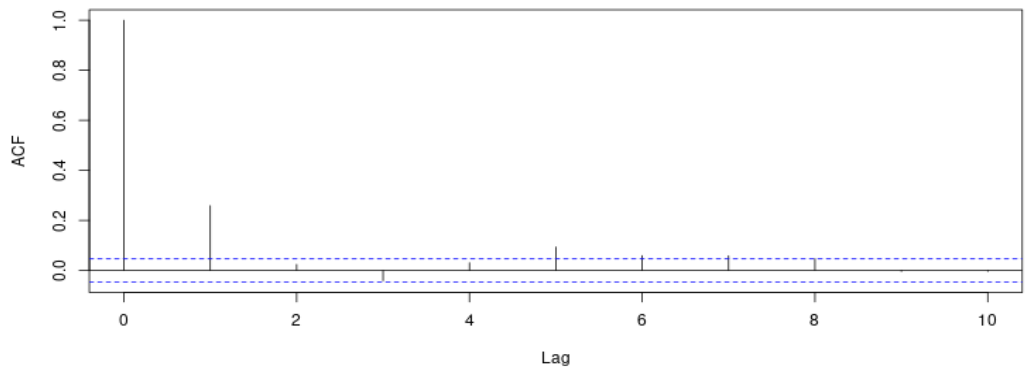

Figure 2.11: Autocorrelation function for the standardized inrements of W.

tion function for up to 10 lags for the standardized increments of the postulated Brownian motion W, where we note that these increments do not show major correlations despite using for the given monthly data approximations which can be expected to cause, due to their construction, some dependency between neighboring increments. Forthcoming work will demonstrate by using daily data that the respective autocorrelation function shows significantly smaller correlation between neighboring increments and practically no correlation between monthly increments. Additionally, we calculated the kurtosis for the above standardized increments and obtained the estimate 3.9, which is close to the kurtosis of standard Gaussian distributed random variables. Since a Brownian motion is defined

as a process with independent Gaussian increments, it appears that the postulated Brownian motion path is most likely difficult to reject as that of a true Brownian motion. It is beyond the scope of this paper to perform rigorous statistical testing in this respect. However, forthcoming work will use daily S&P500 data for showing with high significance that with approximately the same parameters that we estimated in the current paper from monthly data one cannot easily reject the hypothesis that the extracted daily observed path of the postulated Brownian motion is that of a true Brownian motion.

3 Links to the Literature

Historically, the standard continuous time market model for a stock index has been the Black-Scholes model; see Black & Scholes (1973). Its popularity is mostly due to its excellent tractability, however in reality, volatility is stochastic and log-returns have leptokurtic distributions; see e.g. Ghysels, Harvey & Renault (1996). As long-term index model the Black-Scholes model and many of its generalizations are not well-suited because the variance of the logarithm of the index grows linearly, whereas in reality, it appears to remain somehow bounded, as visually indicated by Figure 2.2. Various models have been proposed for the pricing and hedging of index derivatives with maturities of up to about three years. In the following we refer to a few strands of this rich literature to point at links to the proposed new model class.

Engle (1982) initiated extensive research on autoregressive conditional heteroscedastic time series models, with parameters typically depending on the given observation frequency. Continuous time models, characterized by stochastic differential equations (SDEs), avoid this dependency and remain meaningful under different observation frequencies. They can be conveniently handled via the rules of stochastic calculus. Some time series models have similarities with the proposed model for market activity. In particular, squares of 'innovations' and their moving average appear as elements in some time series volatility models.

Nelson (1990) shows that some continuous time limit of an ARCH model yields a volatility process that is driven by a Brownian motion which turns out to be independent of the one driving the index fluctuations. This independence is the opposite to what the proposed model suggests, where only one single Brownian motion is driving the index value and also its volatility. The above fitted proposed model shows perfect negative correlation between the Brownian motions driving the index and its volatility. Under the proposed model the index fluctuations act as signals for the changes in market activity, which makes economic sense because investors reallocate stock holdings according to their strategies when the index changes its value. Furthermore, the well-known leverage effect of equity indexes, see Black (1976), is in many papers artificially introduced and not endogenously generated, whereas the 'normal' volatility emerges endogenously under the proposed model and generates in a natural manner a leverage effect.

The literature suggests a wide range of continuous time stochastic volatility models, where a systematic overview is given, e.g., in Cont (2010). The proposed model can be interpreted as a stochastic volatility model. Its stylized version, the 3/2 model, emerges when the market activity is set to a constant. This is then a local volatility function model because the volatility is here a function of index value and time. Local volatility function models played an important role in the development of quantitative methods for derivatives; see e.g. Dupire (1993). More precisely, the stylized version of the proposed model can be interpreted as a constant elasticity of variance (CEV) model, which belongs to a class of models that goes probably back to Cox (1975).

Due to its random market time, the proposed model is also related to the wide class of subordinated models, which can be traced back to Bochner (1955) and Clark (1973). Here the dynamics of the index evolve in some transformed time, generalizing the Black & Scholes (1973) model.

The proposed model is different to most models that aim directly at modeling stochastic volatility, e.g. the widely used Heston (1993) model. The Heston model became popular due to its excellent tractability. However, over time serious shortcomings were observed, detailed e.g. in Cont (2010). As a consequence, other models became popular among traders, in particular the SABR model; see Hagan et al. (2002). This model evolved among practitioners who aimed for better calibration to market observed derivative prices while maintaining reasonable tractability.
The SABR model is deemed to reflect better volatility effects encapsulated in observed index derivative prices than the Heston model does. Not by chance has the popular SABR model similarities with the model proposed in the current paper. Both models can be interpreted as CEV models that evolve in some random time. Different to the proposed model, the 'market activity' of the SABR model is a geometric Brownian motion. Consequently, the variance of this 'market activity' and the resulting squared volatility grow approximately proportionally to time, which is not what one observes when studying index data over long time periods; see e.g. Figure 2.2. In reality, one observes some mean-reverting behavior of squared volatility. The SABR model remains an 'ad hoc' model, designed for pricing and hedging short-dated derivatives. It is not suitable for realistic long-term modeling of stock indexes.
Most versions of the CEV model make the volatility a function of the underlying, which is in the long-run not realistic because a stock index grows in the long-run and with it under a typical CEV model also the squared volatility, which is not observed in reality. The stylized version of the proposed model (subordinated by deterministic market time with constant market activity) is equivalent to the 3/2 volatility model; see Platen (1997) and Heston (1997).
Many of the above mentioned stochastic volatility models, including the SABR model, assume correlated Brownian motions driving the index and its volatility. As mentioned earlier, Ait-Sahalia, Fan & Li (2013) point at the difficulties

in estimating the correlation between these two Brownian motions, which they call the *leverage effect puzzle*. The reason is that, in reality, one usually does not observe directly the volatility and only the estimated volatility. When the hidden volatility value is linked to an observable quantity, like the normalized index in the proposed model, there is a chance to extract the hidden volatility. The proposed model resolves the leverage effect puzzle by making the usually hidden volatility observable as a function of the normalized index and the market activity. Moreover, it is demonstrating that only one Brownian motion is needed to explain the paths of the index and its hidden volatility, which makes the proposed model class parsimonious. To place index volatility modeling into a more general context, broader than the one considered so far, Section 5 discusses below various alternative volatility models where the usually hidden volatility is made observable as a consequence of the model design similar to the one of the proposed model.

In recent years variance swaps and derivatives on the volatility index (VIX) of the S&P500 became heavily traded, which revealed shortcomings in popular index models; see e.g. Grünbichler & Longstaff (1996), Mencia & Sentana (2013) and Detemple & Kitapbaev (2018). As a consequence, versions of the 3/2 volatility model became popular, which are close to the stylized version of the proposed model; see e.g. Carr & Sun (2007). Moreover, Goard & Mazur (2013) show that a 3/2 volatility model provides a better fit to traded VIX and volatility derivatives than most popular models. Furthermore, Mencia & Sentana (2013) point out that a 3/2 volatility model reproduces naturally the observed positive skew of implied volatilities of VIX options, which is considered to be the most relevant stylized empirical feature of VIX derivatives that has been puzzling traders. Since the proposed model is, in market time, a 3/2 volatility model, this important feature is consistent with the proposed model.
In Baldeaux, Ignatieva & Platen (2014) a time dependent constant elasticity of variance model has been proposed, which generalizes the 3/2 model. By combining the 3/2 and the Heston model, Grasselli (2017) developed an even more general model, the 4/2 volatility model, which has high tractability and fits well derivative data; see Baldeaux, Grasselli & Platen (2014). Moreover, there has been an increasing literature evolving on the theoretical understanding and quantitative methods for the 1/2 (see Heston (1993)), 3/2 and 4/2 models, where we refer to Detemple & Kitapbaev (2018) for important results.
In recent years the availability of high-frequency data revealed that with high-frequency estimated index volatility shows trajectories that appear to be much rougher than typical diffusion models would be able to produce; see e.g. Bayer, Friz & Gatheral (2016) and Gatheral, Thibault & Rosenbaum (2018). The proposed model offers an answer to the question how the roughness of volatility emerges. It suggests that rough volatility is a natural consequence of rough market activity, which can be interpreted as a behavioral response in trading activity to observed fluctuations of the index. More precisely, the proposed model sug-

gests that the index dynamics evolves in market time as that of a diffusion, where in periods of major index moves the market activity (and with it the volatility) spikes when viewed in calendar time because the market time evolves during these periods significantly faster.
Under the proposed model there is no need for introducing any long- or short-range dependence using fractional Brownian motion, which would make the development of practicable quantitative methods extremely challenging. Fortunately, the proposed model is a one-factor, three-component diffusion model in some market time. The market time is accelerated when the index moves. When viewing the diffusion dynamics in calendar time this acceleration appears to capture realistically the roughness of volatility. When estimating the Hurst exponent from rough volatility data for a potential Brownian motion that drives a volatility model in calendar time, then an estimated value can be expected that is clearly different to 0.5, the typical value for a Brownian motion. However, this does not mean that one has to model volatility using some respective fractional Brownian motion which would make respective quantitative methods rather challenging and create potentially some theoretical form of arbitrage.

There exists extensive work on volatility models that involve fast and slow moving components; see Fouque, Papanicolau & Sircar (2000). The proposed model generates fast and slow moving volatility components endogenously. The slow moving component is the 'normal' volatility, which results from the movements of the normalized index in market time. The fast moving component is the market activity, which is a linear function of the square of the derivative of the moving average of a proxy of the driving Brownian motion. Since the Brownian motion path is not differentiable, the market activity can raise to extremely high values at periods when the Brownian motion moves dramatically.
The literature provides a wide range of models that allow for jumps, including exponential Lévy process models and jump diffusion models; see e.g. Barndorff-Nielsen & Shephard (2001) and Bakshi, Cao & Chen (1997). We demonstrate with the proposed model that many movements that one may believe to observe as jumps in estimated volatilities can be explained as being endogenously generated through spikes of market activity. Such sudden spikes are naturally caused by major moves of the driving Brownian motion and the resulting acceleration of market time. Straightforward extensions of the proposed model can easily accommodate jumps caused by particular events, e.g. similarly as in Bakshi, Cao & Chen (1997). Non-decreasing Lévy processes can be incorporated as substitute for the t-time in the proposed model class, making a time transformed driving Brownian motion a Lévy process martingale similar as in Barndorff-Nielsen & Shephard (2001).

Most models in the literature assume the existence of an equivalent risk-neutral probability measure under classical no-arbitrage assumptions; see e.g. Ross (1976),

Harrison & Kreps (1979) and Delbaen & Schachermayer (1994). These assumptions become too restrictive when modeling long-term stock index dynamics, as argued in Platen (2002), Platen & Heath (2010) and Baldeaux, Ignatieva & Platen (2018). The benchmark approach avoids these restrictive assumptions. It requires instead only the existence of the growth optimal portfolio (GP), which is the portfolio that maximizes expected logarithmic utility and goes back to Kelly (1956). The benchmark approach uses the GP as benchmark and numeraire. All benchmarked (in units of the GP denominated) nonnegative securities form supermartingales under the real-world probability measure. Under the stylized version of the proposed model the Radon-Nikodym derivative of the putative risk-neutral measure (the benchmarked savings account) emerges as the inverse of a time transformed squared Bessel process of dimension four, which is an example for a non-negative local martingale that is not a true martingale and, thus, a strict supermartingale; see Revuz & Yor (1999) and Baldeaux, Ignatieva & Platen (2018). Therefore, it is not a true martingale, which the classical risk-neutral assumptions would require. In the sense of Loewenstein & Willard (2000) this causes a money market bubble, see Baldeaux, Ignatieva & Platen (2018), which constitutes a weak form of classical arbitrage. Under the proposed model there is no economically meaningful arbitrage in the pathwise sense that the in the long-run best performing portfolio, the GP, has a finite value at any finite time. Thus, no market participant can generate infinite wealth over any finite time period from finite initial capital.

Under the benchmark approach, see Platen & Heath (2010), which generalizes the classical no-arbitrage approach, one can perform consistently pricing, hedging, portfolio optimization, expected utility maximization and other risk-management tasks. Under the proposed model new effects appear in the financial market dynamics, which can be exploited and are not captured under classical risk-neutral assumptions. In particular, payoffs for long-term pension and life-insurance contracts can be less expensively produced than is possible under the classical no-arbitrage approach using the stylized version of the proposed model; see Platen & Heath (2010).

4 Derivation of the Proposed Model

Within this section we derive the proposed model based on three well-founded assumptions. We emphasize that this model is not another 'ad hoc' model that is chosen for tractability. Due to its derivation from 'first principles' it becomes parsimonious and a rather accurate reflection of reality.

4.1 Index as Growth Optimal Portfolio

We deliberately model the dynamics of a well-diversified stock index and not that of a stock price or an exchange rate because such an exchange price depends on two underlyings, reflecting both sides of the exchanged securities. The diversification that is taking place when forming a well-diversified stock index removes the specific or idiosyncratic uncertainties of stocks. For increasing number of stocks it remains asymptotically the nondiversifiable uncertainty of the respective stock market that drives the value of the stock index.

Diversification theorems have been established in Platen (2005), Platen & Heath (2010) and Platen & Rendek (2012). These allow us to conclude under extremely weak assumptions that a well-diversified stock index with a large number of constituents approximates the GP. This model independent property of well-diversified stock indexes can be interpreted as a consequence of the Law of Large Numbers; see Platen & Rendek (2012). It provides the crucial link between risk and reward, typical for the GP, for the index dynamics.
For a continuous stock market model, where we do not include the locally risk-free asset in the investment universe, it follows by a combination of Theorem 5.1 and Theorem 3.1 in Filipović & Platen (2009) that the value S_{τ_t} of the GP satisfies an SDE of the form

$$\frac{dS_{\tau_t}}{S_{\tau_t}} = \ell_t dt + \theta_{\tau_t}(\theta_{\tau_t} d\tau_t + dW_{\tau_t}) \tag{4.1}$$

$t \geq 0$, $S_0 > 0$. Here $W = \{W_\tau, \tau \geq 0\}$ is a Brownian motion with respect to some strictly increasing market time process $\tau = \{\tau_t, t \geq 0\}$ on a filtered probability space $(\Omega, \mathcal{F}, \underline{\mathcal{F}}, P)$. $\underline{\mathcal{F}} = (\mathcal{F}_t)_{t\geq 0}$ is a filtration, modeling the evolution of information, satisfying the usual conditions; see Karatzas & Shreve (1998). P denotes the real-world probability measure. The 'normal' volatility θ_t is the volatility with respect to market time and forms an adapted process. The excess growth rate ℓ_t forms another adapted process, representing a Lagrange multiplier process.

Since real (inflation adjusted) values matter economically most in the long-term, we consider the index value S_{τ_t}, which is the value at time t of the real-value total return index where the consumer price index is used for denomination. When displaying in Figure 2.2 the logarithm of the standardized real-value S&P500 total return index one notes that it fluctuates around a seemingly straight line, which supports assuming ℓ_t to be constant. This is important, since any drift parameter in an SDE needs an extremely long observation window to become estimated reasonably accurately. To have a realistic chance to estimate the long-term average of the excess growth rate with some accuracy it is helpful to substitute in the proposed model the excess growth rate ℓ_t by its time average denoted by ℓ. This

leads us to our first assumption:

Assumption 4.1 *A well-diversified real-value index follows the dynamics of the respective GP, satisfying the SDE* (4.1)*, where we assume a constant excess growth rate.*

Note that the SDE (4.1) for the GP shows a crucial link between its drift and its diffusion coefficient which relates risk and reward. This link guides us to form the normalized index as

$$Y_{\tau_t} = \frac{S_{\tau_t}}{A_{\tau_t}} = \frac{\tilde{S}_{\tau_t}}{e^{\tau_t}}, \tag{4.2}$$

where we use for normalization the exponential function

$$A_{\tau_t} = A \exp\{\tau_t + \ell t\} \tag{4.3}$$

for $t \geq 0$, with $A > 0$, which gives equation (1.2) of the model. On the far right of (4.2) appears the standardized index

$$\tilde{S}_{\tau_t} = \frac{S_{\tau_t}}{A} \exp\{-\ell t\}, \tag{4.4}$$

satisfying by the Itô formula the SDE

$$\frac{d\tilde{S}_\tau}{\tilde{S}_\tau} = \theta_\tau(\theta_\tau d\tau + dW_\tau) \tag{4.5}$$

for $\tau \geq 0$. We note that when θ is in τ-time a given process, then the normalized index $Y_\tau = \tilde{S}_\tau e^{-\tau}$, see (4.2), emerges as a process in τ-time satisfying by the Itô formula the SDE

$$dY_\tau = Y_\tau(\theta_\tau^2 - 1)d\tau + Y_\tau \theta_\tau dW_\tau \tag{4.6}$$

for $\tau \geq 0$. This provides us with a model structure where the index value is the product of some process value Y_τ and some exponential type function A_τ that captures the average index growth when Y is ergodic. Note, by modeling θ_τ one is not only modeling the volatility of Y_τ with respect to the market time τ but also those of the real-value index and the currency denominated index.

4.2 Variance of Well-Diversified Wealth Increments

The challenge is now to understand the nature of the 'normal' volatility θ_τ in (4.6), which is the volatility of a normalized, well-diversified index with respect to market time. This leads us to the question: What is the natural evolution of the variance of the increments of a normalized, well-diversified index? We make the crucial observation that the value of a normalized, well-diversified portfolio evolves similarly to the size of a normalized population where the individuals give independently birth from time to time or die. This powerful interpretation of diversified wealth evolution appears to be new and is for the first time exploited in this paper.

Birth-and-death processes, also called branching processes, and their diffusion limits are well studied in the literature; see e.g. Feller (1971). To illustrate the similarity between the evolution of the population size of a birth-and-death process and that of a well-diversified index, let us invest at the beginning of a short investment period the index value (the population size) in wealth units of standard size (the individuals). Each of these wealth units generates independent wealth increments (births and deaths). Due to the independence of these wealth increments the variance of the increment of the total wealth (the population size) equals the sum of the variances of the individual wealth increments. Hence, the variance of the increment of the total wealth turns out to be proportional to the number of wealth units invested at the beginning of the short investment period. This means, the variance of the index increments is proportional to the index value itself. At the end of each short time period wealth becomes reallocated such that the total wealth is portioned again into standard wealth units that then evolve independently. This reallocation of wealth represents an activity that one could call diversification. We will see that diversification is not only crucial for the approximation of the GP, see Platen & Rendek (2012), but also for the generation of the feedback effect in the variance of short-term increments of well-diversified wealth. One can deduce the diffusion coefficient of the SDE for the respective continuous time diffusion limit for the normalized index using, e.g., Theorem 14.1.5 in Kloeden & Platen (1999). Since the variance of the index increments is proportional to the index value, the diffusion coefficient of the SDE for the index is proportional to the square root of the index value. This insight leads us to the following assumption:

Assumption 4.2 *The squared diffusion coefficient of a normalized, well-diversified index evolves, in some market time, proportional to the normalized index value.*

Since the market time has so far not been fixed, the diffusion coefficient in (4.6) can be set, without loss of generality, to $Y_\tau \theta_\tau = \sqrt{Y_\tau}$. Therefore, the 'normal' volatility θ_τ, which is the volatility with respect to the market time τ, emerges as

$$\theta_\tau = Y_\tau^{-\frac{1}{2}} \tag{4.7}$$

for $\tau \geq 0$. By using (4.6) this derives the SDE (2.2) for the normalized index.

4.3 Feedback in Market Activity

The changes of the market time τ_t are captured by its derivative, the market activity $M_t = \frac{d\tau_t}{dt}$; see equation (2.4). From (4.5) we obtain by application of the Itô formula the market time τ_t for $t \geq 0$ as given in (2.12). We show in Figure 2.2 the estimated market time $\hat{\tau}_t$ and note that the market activity M_t is fluctuating considerably in periods of major index moves, as those during the Great Depression around 1929. More precisely, we observe that when W_{τ_t} deviates markedly from its recent average level, the market activity increases. Intuitively, this happens because the typical trading behavior of market participants is such that they adjust their holdings according to their respective investment strategies when the index moves, which is typically due to some incoming information.
According to (2.24), W_{τ_t} fluctuates like $2Y_{\tau_t}^{\frac{1}{2}}$ and we can approximate the recent average level of these fluctuations by the moving average U_t of $2Y_{\tau_t}^{\frac{1}{2}}$, where

$$U_t' = \frac{dU_t}{dt} = \lambda(2Y_{\tau_t}^{\frac{1}{2}} - U_t) \tag{4.8}$$

for $t \geq 0$, with $U_0 = 2Y_0^{\frac{1}{2}}$, $\lambda > 0$. This provides equation (2.6) of the proposed model.
The derivative U_t' is an indicator for the magnitude of changes in W. The challenge is now to capture the typical feedback effect in market activity, preferably as a function of the derivative U_t'. Straightforward empirical studies, using polynomials of U_t' as functions for M_t, reveal that the market activity is approximately a linear function of the square of the derivative U_t'. The discovery of this remarkable fact leads us to the following assumption:

Assumption 4.3 *The market activity M_t is a linear function of the square $(U_t')^2$ of the derivative of the moving average of $2Y_{\tau_t}^{\frac{1}{2}}$.*

Under Assumption 4.3 we obtain for the proposed model the market activity in the form given in (2.5).
From a quantitative perspective one may ask for some intuitive explanation for the surprisingly good fit between the integrated model market activity (the model market time) and the estimated market time in Figure 2.7. Why are the movements of the estimated market time almost all reflected by movements of the model market time? Note that the estimated market time is close to the quadratic variation of $2Y_{\tau_t}^{\frac{1}{2}}$. The latter is approximated by the sum over the squared differences $(2Y_{\tau_{t_i}}^{\frac{1}{2}} - 2Y_{\tau_{t_{i-1}}}^{\frac{1}{2}})^2$. This sum evolves similarly to the sum over the squared differences $(2Y_{\tau_{t_i}}^{\frac{1}{2}} - U_{t_i})^2$, which yields approximately the integrated model market

activity when neglecting the base activity. In some sense U_{t_i} plays here the role that $2Y^{\frac{1}{2}}_{\tau_{t_{i-1}}}$ plays in the approximate quadratic variation.

One may ask whether there exist more accurate functional relationships for the dependence of M_t on $U_t^{'}$? This can be indeed expected to be the case, as already indicated towards the end of Subsection 2.4 and will be demonstrated in forthcoming work. We propose in the current paper a simple linear functional relationship for the market activity on $U_t^{'}$ as a starting point. It gives us a first understanding of the origins of stochastic volatility and its roughness. This functional relationship can be refined and modified for different indexes and time periods depending on the average aggregate trading behavior of the respective market participants as a response to index moves. The derived model class opens a direction for interesting future research.

4.4 Existence and Uniqueness

Finally, we conclude the derivation of the model by ensuring the existence and uniqueness of a strong solution of the system of SDEs characterizing the model: The existence and uniqueness of a strong solution of the SDE (2.2) for the normalized index in market time follows by using the well-known Yamada-condition; see Ikeda & Watanabe (1989). The differential equation (2.6) for the moving average U can be shown to have in market time a continuous solution with bounded derivative of its drift function. Thus, it satisfies a Lipschitz condition and has, therefore, a unique, strong solution in τ-time; see Ikeda & Watanabe (1989). Consequently, the system of model SDEs with respect to market time has a unique, strong solution. Since the market activity in equation (2.5) is strictly positive and by (2.6) a function of U, the calendar time t is uniquely determined in the strong sense of Ikeda & Watanabe (1989). Thus, the proposed system of model SDEs, when evolving in t-time, has a unique, strong solution because t-time and τ-time are uniquely linked by the market activity; see (2.4).
The above discussion makes also clear that the evolution of the normalized index in τ-time forms the core of the model dynamics. The market activity and with it the t-time can be interpreted as a 'consequence' of this evolution. This may seem a bit surprising. However, when recalling that a diversified wealth evolution has deep similarities with that of a birth and death process, then it becomes clear that in times when more births and deaths occur, which means in our setting trading is more active, the dynamics run faster. The market participants speed up or slow down market time through their response in trading activity to fluctuations of the index. This response causes the observed spikes and roughness in volatility, which are a result of the accelerated, much faster market evolution in periods when new information arrives that moves the stock prices and, thus, the driving Brownian motion away from its recent average level. Interesting is here

that the average response in market activity to Brownian motion fluctuations seems to be rather stable over long periods of time, which allows us to extract a simple functional relationship for the market activity. Forthcoming research will show that the time dependent modeling of intraday, seasonal and business cycle driven changes of the activity scale improves the fit of the model market time to the estimated market time. Such time dependence, when sensibly modeled, does not jeopardize the existence and uniqueness of the model dynamics of the proposed model class.

5 Various Volatility Models

Let us now consider a broader range of volatility models than the one derived above. This section discusses modifications of various popular volatility models for modeling in some market time the normalized index dynamics. We employ in this section only one Brownian motion to keep the model classes we consider parsimonious. We consider below models analogous to the derived model, where we substitute the 'normal' volatility dynamics by those of popular volatility models. We then check whether any of the alternative model classes could reflect realistically stylized empirical facts observed for stock indexes. We will see that in our setting, where we model the dynamics of a GP driven by one Brownian motion, the respective 'normal' volatility has to satisfy an important drift condition.

5.1 Drift Condition for 'Normal' Volatility

By keeping in the remainder of this section our Assumption 4.1 valid we obtain for the following classes of alternative models the equations (4.2) to (4.6). Instead of imposing Assumption 4.2, let us specify more generally the dynamics of the 'normal' volatility θ_τ in a way that accommodates various popular volatility models. We assume for the 'normal' volatility θ_τ the SDE

$$d\theta_\tau = \mu(\theta_\tau)\, d\tau + \psi(\theta_\tau)\, dW_\tau, \tag{5.9}$$

where W_τ denotes the value of the single driving Brownian motion in τ-time. Furthermore, the drift coefficient function $\mu(.)$ and the diffusion coefficient function $\psi(.)$ in (5.9) are assumed to be suitable differentiable functions of the 'normal' volatility θ_τ so that a unique strong solution for the SDE (5.9) exists and the manipulations we perform below are well-defined.
In the special case when we have $\psi(.) = 0$ the 'normal' volatility is a deterministic function of τ-time and we end up with a Black & Scholes (1973) type dynamics for the GP in τ-time. Note that other models with deterministic volatility include those employed in Föllmer & Schweizer (1993), Platen & Rebolledo (1996) and Fleming & Sheu (1999). Since for nonvanishing $\theta_\tau > \tilde{\epsilon} > 0$ the variance of

the logarithm of the GP increases with τ, which is not the case in reality and can be seen in Figure 2.2, we can dismiss the above mentioned type of models as suitable long-term models for the GP and assume for the remainder of this section $\psi(.) > 0$.

As is the case for the derived model, we consider only models where the normalized GP $Y_\tau = Y(\theta_\tau)$ is a function of the 'normal' volatility θ_τ and vice versa. The following theorem reveals that this restricts the class of possible models considerably:

Theorem 5.1 (Normalized GP Formula) *For a differentiable diffusion coefficient function $\psi(\theta)$ of the 'normal' volatility the corresponding normalized GP value is given by the formula*

$$Y(\theta) = \exp\left\{\int_{\bar{\theta}}^{\theta} u\psi(u)^{-1}du\right\} \tag{5.10}$$

for some $\bar{\theta} > 0$ and every $\theta > 0$, assuming $\theta\psi(\theta)^{-1}$ to be integrable with respect to θ, and $Y(.)$ strictly positive and twice differentiable.

Proof: For a function $a(.)$ let $a'(.)$ and $a''(.)$ denote its derivative and second derivative, respectively. It follows by the Itô formula for the normalized GP the SDE

$$dY_\tau = Y'(\theta_\tau)d\theta_\tau + \frac{1}{2}Y''(\theta_\tau)d[\theta_.]_\tau. \tag{5.11}$$

By comparing the diffusion term in (5.11) with that in (4.6) we obtain the equation

$$Y'(\theta)\psi(\theta) = Y(\theta)\theta \tag{5.12}$$

for all $\theta > 0$. Thus, we have

$$\frac{Y'(\theta)}{Y(\theta)} = \frac{\theta}{\psi(\theta)}, \tag{5.13}$$

which proves formula (5.10). Note that the function $\theta\psi(\theta)^{-1}$ is assumed to be integrable with respect to θ. □

The above result is a consequence of the fact that the diffusion coefficient of the normalized GP in the SDE (4.6) is linked to its drift coefficient in a way that only involves the 'normal' volatility.

Another consequence of the above revealed link is a surprising *volatility drift condition* for the 'normal' volatility, which we provide in the following theorem:

Theorem 5.2 (Volatility Drift Condition) *Under the assumptions of Theorem 5.1 the drift coefficient function of the SDE* (5.9) *is fully determined and*

given by the formula

$$\mu(\theta) = \frac{\psi(\theta)}{2\theta}(\theta^2 - 2 - \psi(\theta) + \theta\psi'(\theta)) \tag{5.14}$$

for $\theta > 0$.

Proof: From (5.12) and (5.10) it follows the first derivative of $Y(\theta)$ in the form

$$Y'(\theta) = Y(\theta)\theta\psi(\theta)^{-1} \tag{5.15}$$

for $\theta > 0$. Thus, the second derivative of $Y(\theta)$ equals

$$Y''(\theta) = Y'(\theta)\theta\psi(\theta)^{-1} + Y(\theta)\psi(\theta)^{-1} - Y(\theta)\theta\psi(\theta)^{-2}\psi'(\theta). \tag{5.16}$$

For the SDE (5.11) we obtain with (5.12), (5.16) and (5.11) according to (4.6) its drift function, satisfying the equality

$$Y(\theta)(\theta^2 - 1) = Y(\theta)\theta\psi(\theta)^{-1}\mu(\theta) + \frac{1}{2}(Y(\theta)\theta^2 + Y(\theta)\psi(\theta) - Y(\theta)\theta\psi'(\theta)). \tag{5.17}$$

Thus, the drift function for the SDE of the 'normal' volatility has the form

$$\mu(\theta) = \psi(\theta)\theta^{-1}(\theta^2 - 1 - \frac{1}{2}(\theta^2 + \psi(\theta) - \theta\psi'(\theta))), \tag{5.18}$$

which confirms formula (5.14). □

The above drift condition is somehow surprising when recalling that most of the literature does not impose restricions in the drifts of volatility dynamics. Still, the above volatility drift condition seems to have some similarity with the seminal Heath-Jarrow-Morton drift condition for forward rates. The latter was derived under an assumed risk-neutral probability measure; see Heath, Jarrow & Morton (1992). In Section 10.4 of Platen & Heath (2010) a similar condition was derived for forward rates under the real-world probability measure. The above volatility drift condition follows under the real-world probability measure. It is a drift condition for the volatility of the index dynamics, more precisely, the GP dynamics with respect to market time. By chosing a respective diffusion coefficient function for the SDE of the 'normal' volatility, one can cover a wide range of popular Markovian 'normal' volatility models.

5.2 p-Volatility Models

A large group of classes of volatility models proposed in the literature, which we call here *p-volatility models*, can be classified by the exponent p of a power function in the diffusion coefficient of the squared 'normal' volatility $(\theta_\tau)^2$. To be precise, let us characterize the diffusion coefficient in the SDE (5.9) for the

'normal' volatility by some finite exponent p and a scaling parameter $\gamma \neq 0$ in the form

$$\psi(\theta) = \gamma\theta^{2p-1}. \tag{5.19}$$

By application of the Itô formula we obtain from (5.9) with (5.19) and (5.14) for the squared 'normal' volatility the SDE

$$d(\theta_\tau)^2 = \gamma((\theta_\tau)^2)^{p-\frac{1}{2}}\left((\theta_\tau)^2 - 2 + \gamma(2p-1)((\theta_\tau)^2)^{p-\frac{1}{2}}\right)d\tau + 2\gamma\left((\theta_\tau)^2\right)^p dW_\tau \tag{5.20}$$

for $\tau \geq 0$ with $(\theta_0)^2 > 0$.

1/2-Volatility Model

By setting $p = 1/2$ we obtain from (5.20) for the squared 'normal' volatility the *1/2-volatility model* with SDE

$$d(\theta_\tau)^2 = \gamma\left((\theta_\tau)^2 - 2\right)d\tau + 2\gamma\left((\theta_\tau)^2\right)^{\frac{1}{2}} dW_\tau. \tag{5.21}$$

This model makes sense in the long-term when one sets $\gamma < 0$, which generates a leverage effect as observed in reality. The drift is then also linear mean-reverting, which is generating stable long-term dynamics. The model can be identified as a Heston model, where $(\theta_\tau)^2$ follows a square root process of dimension $-2/\gamma$. Since only models are suitable for long-term modeling when the squared 'normal' volatility remains strictly positive, the dimension of this square root process has to be greater than 2 and, thus, γ needs to be between -1 and 0, which is an important restriction.

By Theorem 5.1, for the 1/2-volatility model the normalized GP is a function of the 'normal' volatility given by the formula

$$Y(\theta) = \exp\left\{\frac{1}{2\gamma}(\theta^2 - \bar{\theta}^2)\right\} \tag{5.22}$$

for $\theta > 0$. By inverting the above function $Y(\theta)$ we obtain from (4.6) for Y_τ the SDE

$$dY_\tau = Y_\tau(2\gamma\ln(Y_\tau) + \bar{\theta}^2 - 1)d\tau + Y_\tau(2\gamma\ln(Y_\tau) + \bar{\theta}^2)^{\frac{1}{2}}dW_\tau. \tag{5.23}$$

This SDE reveals that the model can be interpreted as a local volatility function model with local volatility function

$$\theta(Y) = (2\gamma\ln(Y) + \bar{\theta}^2)^{\frac{1}{2}} \tag{5.24}$$

for $Y > 0$. It would be not appropriate for a long-term model to make the local volatility a function of the underlying index. Instead, we obtain it it here more realistically as a function of the normalized GP Y_τ. What makes the Heston model tractable is the fact that the squared volatility of the GP forms a square

root process and the normalized GP value is a function of this process; see (5.22). The square root process θ^2 for the squared 'normal' volatility has as stationary density a gamma density with $-2/\gamma$ degrees of freedom. When estimating the distribution of short-term log-returns, then one can expect to observe under the 1/2-volatility model the effect of a normal mixture distribution, where the variance of the returns is gamma distributed with $-2/\gamma$ degrees of freedom. Thus, under the Heston model one would observe variance gamma distributed returns. This is not what one observes in reality; see e.g. Platen & Rendek (2008). The 1/2-volatility or Heston model does not match this important stylized empirical fact.

1.0-Volatility Model

For the exponent parameter $p = 1$ the squared volatility has a multiplicative diffusion coefficient as it arises, e.g., for a geometric Brownian motion. This type of diffusion coefficient for squared volatility is typical when modeling squared volatility as exponential of an Ornstein-Uhlenbeck process; see e.g. Wiggins (1987), Chesney & Scott (1989) and Melino & Turnbull (1990). Furthermore, the continuous time limit of some ARCH models yield multiplicative diffusion coefficients for the squared volatility; see e.g. Nelson (1990) and Frey (1997). However, in Nelson (1990) the Brownian motion driving the volatility turns out to be independent from the one driving the underlying index, whereas for the derived model it is perfectly negatively correlated.

For the choice $p = 1$ we obtain from (5.20) for the squared 'normal' volatility the SDE

$$d(\theta_\tau)^2 = \gamma((\theta_\tau)^2)^{\frac{1}{2}} \left((\theta_\tau)^2 - 2 + \gamma((\theta_\tau)^2)^{\frac{1}{2}} \right) d\tau + 2\gamma(\theta_\tau)^2 dW_\tau. \tag{5.25}$$

By formula (5.10) we can express the normalized index value as

$$Y(\theta) = \exp\left\{ \frac{1}{\gamma}(\theta - \bar{\theta}) \right\}. \tag{5.26}$$

Inverting the above function yields the local volatility function

$$\theta(Y) = (\gamma \ln(Y) + \bar{\theta})^{\frac{1}{2}} \tag{5.27}$$

for $Y > 0$. Thus, from (4.6) we obtain for Y_τ the non-linear SDE

$$dY_\tau = Y_\tau(\gamma \ln(Y_\tau) + \bar{\theta} - 1)d\tau + Y_\tau(\gamma \ln(Y_\tau) + \bar{\theta})^{\frac{1}{2}} dW_\tau. \tag{5.28}$$

One notes that the 1.0-volatility model has a stationary density for $(\theta_\tau)^2$ that is clearly different to an inverse gamma density and, thus, generates returns that in their tails cannot be expected to match well the tails of historical stock index returns.

3/2-Volatility Models

The derived model relates to the exponent $p = 3/2$. We obtain for this choice from (5.20) for the squared 'normal' volatility the SDE

$$d(\theta_\tau)^2 = \gamma(\theta_\tau)^2 \left((2\gamma+1)(\theta_\tau)^2 - 2\right) d\tau + 2\gamma \left((\theta_\tau)^2\right)^{\frac{3}{2}} dW_\tau. \tag{5.29}$$

Since the scaling parameter γ is still a free parameter, we have here obtained a family of 3/2-volatility models. Note that the inverse of the squared 'normal' volatility satisfies the SDE

$$d(\theta_\tau)^{-2} = \left(\gamma(2\gamma-1) + 2\gamma(\theta_\tau)^{-2}\right) d\tau - 2\gamma \left((\theta_\tau)^{-2}\right)^{\frac{1}{2}} dW_\tau, \tag{5.30}$$

which is that of a square root process of dimension $2 - \frac{1}{\gamma}$. To avoid volatility explosion we have to keep the dimension of this square root process beyond 2 and, thus, $\gamma < 0$. This negative scaling parameter γ generates a leverage effect. We obtain by (5.10) the value of the normalized index as a function of the 'normal' volatility in the form

$$Y(\theta) = \left(\frac{\theta}{\bar{\theta}}\right)^{\frac{1}{\gamma}}. \tag{5.31}$$

The inverse function of (5.31) provides the respective local volatility function

$$\theta(Y) = \bar{\theta} Y^\gamma. \tag{5.32}$$

This yields for the class of 3/2-volatility models by (4.6) for the normalized index the SDE

$$dY_\tau = (\bar{\theta}^2 Y_\tau^{2\gamma+1} - Y_\tau) d\tau + \bar{\theta} Y_\tau^{\gamma+1} dW_\tau. \tag{5.33}$$

We can interpret this class as part of the constant elasticity of variance (CEV) model class; see e.g. Cox (1975), Cox (1996), Schroder (1989), Heath & Platen (2002) and Delbaen & Shirakawa (2002). The stationary density of the normalized index is a gamma density with $2 - \frac{1}{\gamma}$ degrees of freedom. Since the modeling of rare, extreme returns is highly relevant for long-term risk management, the appropriate choice for the parameter γ is paramount. To obtain a stationary density of about four degrees of freedom, which would yield estimated returns as observed in reality, one has to set $\gamma \approx -\frac{1}{2}$. However, this yields the above derived model when starting the index with an initial value that yields $\bar{\theta} \approx 1$; see (2.17).

If one considers the popular SABR model in its time scale, see Hagan, Kumar, Lesniewski & Woodward (2002), then it can be interpreted as a CEV-type model. For short-term modeling such CEV-type model has similarities with the derived model, as mentioned earlier. However, for long-term index modeling the SABR model and most CEV-type models proposed in the literature are not well-suited when specifying the local volatility function for the 'normal' volatility as a time

homogenous function of the index value and not as a function of a normalized index value. The volatility needs to exhibit some stationary behavior as it appears to be the case in reality.

2.0-Volatility Model

The choice $p = 2$ for the exponent yields the *2.0-volatility model*. By (5.20) one obtains for its squared 'normal' volatility the SDE

$$d(\theta_\tau)^2 = \gamma \left(((\theta_\tau)^2)^{\frac{5}{2}} - 2((\theta_\tau)^2)^{\frac{3}{2}} + 3\gamma((\theta_\tau)^2)^3 \right) d\tau + 2\gamma \left((\theta_\tau)^2 \right)^2 dW_\tau. \tag{5.34}$$

We obtain by (5.10) for the normalized index value the formula

$$Y(\theta) = \exp\left\{ \frac{1}{\gamma} (\bar{\theta}^{-1} - \theta^{-1}) \right\}. \tag{5.35}$$

Inverting this function yields the respective local volatility function

$$\theta(Y) = (\bar{\theta}^{-1} - \gamma \ln(Y))^{-1} \tag{5.36}$$

for $Y > 0$. Thus, by (4.6) the normalized index satisfies the SDE

$$dY_\tau = Y_\tau (\bar{\theta}^{-1} - \gamma \ln(Y))^{-2} d\tau + Y_\tau (\bar{\theta}^{-1} - \gamma \ln(Y))^{-1} dW_\tau. \tag{5.37}$$

Also here, the stationary density for $(\theta_\tau)^2$ is clearly different to that of the inverse of a gamma distributed random variable. This means, the log-returns that the model generates are different to Student-t distributed log-returns with about four degrees of freedom and, thus, different to those observed in reality.

4/2-Volatility Model

By suggesting a mixture of 1/2- and 3/2-volatility models, Grasselli suggested the highly tractable *4/2-volatility* model; see e.g. Grasselli (2017) and Baldeaux, Grasselli & Platen (2014). It is constructed using a scalar diffusion process V satisfying an SDE of the form

$$dV_\tau = \kappa(V_\tau) d\tau + \rho V_\tau^{\frac{1}{2}} dW_\tau \tag{5.38}$$

with constant $\rho > 0$, where $\kappa(V_\tau)$ is in Grasselli (2017) assumed to be a linear function of V_τ such that V becomes a square root process. The 'normal' volatility is then set to

$$\theta_\tau = a V_\tau^{\frac{1}{2}} + b V_\tau^{-\frac{1}{2}}, \tag{5.39}$$

where for $b = 0$ one obtains a 1/2-volatility model and for $a = 0$ a 3/2-volatility model. When assuming $Y_\tau = \tilde{Y}(V_\tau)$ to be a twice differentiable function of V_τ,

its derivative follows by application of the Itô formula and comparison of the diffusion coefficient with the diffusion coefficient in the SDE (4.6) gives

$$\tilde{Y}'(V) = \tilde{Y}(V)(a + bV^{-1})\frac{1}{\rho}. \tag{5.40}$$

This yields the second derivative of the function $Y(V)$ in the form

$$\tilde{Y}''(V) = \tilde{Y}(V)\left((\frac{a}{\rho} + \frac{b}{\rho}V^{-1})^2 - \frac{b}{\rho}V^{-2}\right). \tag{5.41}$$

By application of the Itô formula to $\tilde{Y}(V_\tau)$ and comparison of the drift coefficient with the drift coefficient in the SDE (4.6) it follows that the drift coefficient function in the SDE (5.38) for V_τ has to be of the form

$$\kappa(V) = \frac{\rho}{2}\left(aV + b + (b\rho V^{-\frac{1}{2}} - V^{\frac{1}{2}})(aV^{\frac{1}{2}} + bV^{-\frac{1}{2}})^{-1}\right). \tag{5.42}$$

Note that we have here again a drift condition in analogy to the volatility drift condition we derived earlier. When modeling the normalized GP dynamics, only in the already previously discussed cases $a = 0$ or $b = 0$, respectively, the function $\kappa(V)$ turns out to be a linear function. In the other cases it becomes non-linear and the in Grasselli (2017) presented 4/2-volatility model is, unfortunately, not adding a new dynamics to the considered broader model class. For $a = 0, b = 1$ and $\kappa(V) = \rho^2(1 - V)$ the derived model emerges.

Generalized 1/2- and 3/2-Volatility Models

Another interesting work on volatility modeling in Detemple & Kitapbaev (2018) suggested and studied generalized model classes that include the highly tractable 1/2- and 3/2-volatility models. The construction of the models starts similarly to the one in Grasselli (2017) by assuming a square root process V of dimension $\delta > 2$ as a factor process given by the SDE

$$dV_\tau = (\frac{\delta}{4}\rho^2 - \omega V_\tau)d\tau + \rho V_\tau^{\frac{1}{2}} dW_\tau \tag{5.43}$$

for $\tau \geq 0$ with $V_0 > 0$, $\rho \neq 0$ and $\omega > 0$. The volatility $\theta_\tau = \theta(V_\tau)$ is then assumed to be a function of the factor V_τ such that an inverse function $g(.)$ of the function $\theta(.)$ exists, where $g(\theta(V)) = V$ and all manipulations performed below make sense.
When applied to our broader setting, by Theorem 5.1 the normalized GP becomes a function of the volatility θ_τ and a function of the factor V_τ. Similarly as in the proof of Theorem 5.1 the normalized index value satisfies then the formula

$$Y_\tau = \bar{Y}(V_\tau) = \exp\left\{\frac{1}{\rho}\int_{\bar{V}}^{V_\tau} \theta(v)v^{-\frac{1}{2}}dv\right\} \tag{5.44}$$

for some $\bar{V} > 0$. By steps analogous to those in the proof of Theorem 5.2, this leads for the SDE (5.43) to the respective *drift condition*

$$\frac{\delta}{4}\rho^2 - \omega V = \frac{\rho}{\theta} V^{\frac{1}{2}} \left(\frac{\theta^2}{2} - 1 - \frac{\rho}{2}\theta' V^{\frac{1}{2}} + \frac{\rho}{4} V^{-\frac{1}{2}} \theta \right), \tag{5.45}$$

which is analogous to the previously derived volatility drift condition.
It is beyond the scope of this paper to search for functions $\theta(.)$ solving the above differential equation. However, we already know that the class of 1/2-volatility models provides such solutions: More precisiely, when setting $\theta(V) = \xi V^{\frac{1}{2}}$ the above drift condition requires for $\rho < 0$, $0 < \omega < 1$ and $\delta = \frac{2}{\omega}$ to set $\xi = -\frac{2\omega}{\rho}$ for obtaining a 1/2-volatility model.
Another family of solutions for the differential equation (5.45) relates to the class that contains the derived model, the class of 3/2-volatility models: When setting $\theta(V) = \phi V^{-\frac{1}{2}}$, the drift condition (5.45) requests for $\rho > 0$, $\omega > 0$ and $\delta = 2(\frac{1}{\omega}+1)$ to set $\phi = \frac{\rho}{\omega}$ for obtaining a 3/2-volatility model. The choice $\omega = 1$ yields the derived model, which among the alternative volatility models considered in this section matches best the empirical evidence provided in Platen & Rendek (2008) on the tail behavior of log-returns.

Conclusion

Based on well-founded assumptions, the paper derives a new model class for the long-term dynamics of well-diversified stock indexes. It proposes a model that fits surprisingly well monthly observed real value S&P500 total return data. The model is driven by only one single Brownian motion, which makes the model parsimonious and captures the non-diversifiable uncertainty of the stock market. The normalized index is modeled as a square root process that evolves in some market time. When viewed in calendar time, the derivative of market time, the market activity, is rough and shows spikes during periods of high market activity. The index is the product of the normalized index and some exponential function of time and market time. The derived model explains naturally rough volatility as a consequence of rough market activity. Moreover, it generates the leverage effect and Student-t distributed log-returns with about four degrees of freedom, as observed in reality. Various alternative popular volatility models do not capture jointly these stylized empirical index properties.
The proposed model class leads beyond the classical risk-neutral approach and is derived under the benchmark approach. The proposed model volatility with respect to market time has perfect negative correlation with the index. Through the proposed model class the, so called, leverage effect puzzle has been resolved, where the correlation between volatility and index seemed inaccessible. Higher-order, implicit stochastic expansions for increments of observed and hidden model components turn out to be necessary for fitting the model to monthly observed

data, extracting the rough market activity and the path of the driving Brownian motion.

References

Ait-Sahalia, Y., J. Fan, & Y. Li (2013). The leverage effect puzzle: Disentangling sources of bias at high frequency. *J. Fin. Economics* **109**, 224–249.

Bakshi, G., C. Cao, & Z. Chen (1997). Empirical performance of alternative option pricing models. *J. Finance* **LII**, 2003–2049.

Baldeaux, J., M. Grasselli, & E. Platen (2014). Pricing currency derivatives under the benchmark approach. *J. Banking Fin.* **53**, 34–48.

Baldeaux, J., K. Ignatieva, & E. Platen (2014). A tractable model for indices approximating the growth optimal portfolio. *Studies Nonl. Dyn. Econometrics* **18**(1), 1–21.

Baldeaux, J., K. Ignatieva, & E. Platen (2018). Detecting money market bubbles. *J. Banking Fin.* **87**, 369–379.

Barndorff-Nielsen, O. & N. Shephard (2001). Modelling by Lévy processes for financial econometrics. In O. E. Barndorff-Nielsen, T. Mikosch, and S. Resnick (Eds.), *Lévy Processes - Theory and Applications*, pp. 283–318. Birkhäuser, Boston.

Bayer, C., P. Friz, & J. Gatheral (2016). Pricing under rough volatility. *Quant. Finance.* **16**(6), 887–904.

Black, F. (1976). Studies in stock price volatility changes. In *Proceedings of the 1976 Business Meeting of the Business and Economic Statistics Section, American Statistical Association*, pp. 177–181.

Black, F. & M. Scholes (1973). The pricing of options and corporate liabilities. *J. Political Economy* **81**, 637–654.

Bochner, S. (1955). *Harmonic Analysis and the Theory of Probability.* University of California Press, Berkeley, CA.

Carr, P. & J. Sun (2007). A new approach for option pricing under stochastic volatility. *Rev. Deriv. Research* **10**, 87–150.

Chesney, M. & L. O. Scott (1989). Pricing European currency options: A comparison of the modified Black-Scholes model and a random variance model. *J. Financial and Quantitative Analysis* **24**, 267–284.

Clark, P. K. (1973). A subordinated stochastic process model with finite variance for speculative prices. *Econometrica* **41**, 135–159.

Cont, R. (2010). *Encyclopedia of Quantitative Finance.* Wiley.

Cox, J. C. (1975). Notes on option pricing I: constant elasticity of variance diffusions. Stanford University, (working paper, unpublished).

Cox, J. C. (1996). The constant elasticity of variance option pricing model. *J. Portfolio Manag.* (Special Issue), 15–17.

Delbaen, F. & W. Schachermayer (1994). A general version of the fundamental theorem of asset pricing. *Math. Ann.* **300**, 463–520.

Delbaen, F. & H. Shirakawa (2002). A note on option pricing for the constant elasticity of variance model. *Asia-Pacific Financial Markets* **9**(2), 85–99.

DeMiguel, V., L. Garlappi, & R. Uppal (2009). Optimal versus naive diversification: How inefficient is the $1/n$ portfolio strategy? *Rev. Financial Studies* **22**(5), 1915–1953.

Detemple, J. & Y. Kitapbaev (2018). On american vix options under the generalized 3/2 and 1/2 models. *Math. Finance* **28**(2), 550–581.

Dupire, B. (1993). Model art. *Risk* **6**, 118–124.

Engle, R. F. (1982). Autoregressive conditional heteroskedasticity with estimates of the variance of U.K. inflation. *Econometrica* **50**(4), 987–1007.

Feller, W. (1971). *An Introduction to Probability Theory and Its Applications* (2nd ed.), Volume 2. Wiley, New York.

Fergusson, K. & E. Platen (2006). On the distributional characterization of log-returns of a world stock index. *Appl. Math. Finance* **13**(1), 19–38.

Filipović, D. & E. Platen (2009). Consistent market extensions under the benchmark approach. *Math. Finance* **19**(1), 41–52.

Fleming, W. H. & S.-J. Sheu (1999). Optimal long term growth rate of expected utility of wealth. *Ann. Appl. Probab.* **9**, 871–903.

Föllmer, H. & M. Schweizer (1993). A microeconomic approach to diffusion models for stock prices. *Math. Finance* **3**, 1–23.

Fouque, J. P., G. Papanicolau, & K. R. Sircar (2000). *Derivatives in Markets with Stochastic Volatility*. Cambridge University Press.

Frey, R. (1997). Derivative asset analysis in models with level-dependent and stochastic volatility. Mathematics of Finance, Part II. *CWI Quarterly* **10**(1), 1–34.

Gatheral, J., J. Thibault, & M. Rosenbaum (2018). Volatility is rough. *Quant. Finance.* **18**(6), 933–949.

Ghysels, E., A. Harvey, & E. Renault (1996). Stochastic volatility. In *Statistical Methods in Finance*, Volume 14 of *Handbook of Statist.*, pp. 119–191. North-Holland.

Goard, J. & M. Mazur (2013). Stochastic volatility models and the pricing of vix options. *Mathematical Finance* **23**, 439–458.

Grasselli, M. (2017). The 4/2 stochastic volatility model. *Math. Finance* **27**(4), 1013–1034.

Grünbichler, A. & F. Longstaff (1996). Valuing futures and options on volatility. *J. Banking Fin.* **20**, 985–1001.

Hagan, P., D. Kumar, A. Lesniewski, & D. Woodward (2002). Managing smile risk. *Wilmott Magazine*, 84–108.

Harrison, J. M. & D. M. Kreps (1979). Martingale and arbitrage in multiperiod securities markets. *J. Economic Theory* **20**, 381–408.

Heath, D., R. Jarrow, & A. Morton (1992). Bond pricing and the term structure of interest rates: A new methodology for contingent claim valuation. *Econometrica* **60**(1), 77–105.

Heath, D. & E. Platen (2002). Consistent pricing and hedging for a modified constant elasticity of variance model. *Quant. Finance.* **2**(6), 459–467.

Heston, S. L. (1993). A closed-form solution for options with stochastic volatility with applications to bond and currency options. *Rev. Financial Studies* **6**(2), 327–343.

Heston, S. L. (1997). A simple new formula for options with stochastic volatility. Technical report, Washington University of St. Louis.

Hurst, S. R. & E. Platen (1997). The marginal distributions of returns and volatility. In Y. Dodge (Ed.), L_1*-Statistical Procedures and Related Topics*, Volume 31 of *IMS Lecture Notes - Monograph Series*, pp. 301–314. Institute of Mathematical Statistics Hayward, California.

Ikeda, N. & S. Watanabe (1989). *Stochastic Differential Equations and Diffusion Processes* (2nd ed.). North-Holland. (first edition (1981)).

Karatzas, I. & S. E. Shreve (1998). *Methods of Mathematical Finance*, Volume 39 of *Appl. Math.* Springer.

Kelly, J. R. (1956). A new interpretation of information rate. *Bell Syst. Techn. J.* **35**, 917–926.

Kloeden, P. E. & E. Platen (1999). *Numerical Solution of Stochastic Differential Equations*, Volume 23 of *Appl. Math.* Springer. Third printing, (first edition (1992)).

Loewenstein, M. & G. A. Willard (2000). Local martingales, arbitrage, and viability: Free snacks and cheap thrills. *Econometric Theory* **16**(1), 135–161.

Markowitz, H. & N. Usmen (1996a). The likelihood of various stock market return distributions, Part 1: Principles of inference. *J. Risk & Uncertainty* **13**(3), 207–219.

Markowitz, H. & N. Usmen (1996b). The likelihood of various stock market return distributions, Part 2: Empirical results. *J. Risk & Uncertainty* **13**(3), 221–247.

Melino, A. & S. Turnbull (1990). Pricing foreign currency options with stochastic volatility. *J. Econometrics* **45**, 239–265.

Mencia, J. & E. Sentana (2013). Valuation of vix derivatives. *Journal of Financial Economics* **108**, 367–391.

Merton, R. C. (1973). Theory of rational option pricing. *Bell J. Econ. Management Sci.* **4**, 141–183.

Merton, R. C. (1992). *Continuous-Time Finance*. Blackwell, Oxford.

Nelson, D. B. (1990). ARCH models as diffusion approximations. *J. Econometrics* **45**, 7–38.

Platen, E. (1997). A non-linear stochastic volatility model. Technical report, Australian National University, Canberra, Financial Mathematics Research Reports. FMRR 005-97.

Platen, E. (2002). Arbitrage in continuous complete markets. *Adv. in Appl. Probab.* **34**(3), 540–558.

Platen, E. (2005). Diversified portfolios with jumps in a benchmark framework. *Asia-Pacific Financial Markets* **11**(1), 1–22.

Platen, E. & N. Bruti-Liberati (2010). *Numerical Solution of Stochastic Differential Equations with Jumps in Finance*. Springer.

Platen, E. & D. Heath (2010). *A Benchmark Approach to Quantitative Finance*. Springer Finance. Springer.

Platen, E. & R. Rebolledo (1996). Principles for modelling financial markets. *J. Appl. Probab.* **33**, 163–172.

Platen, E. & R. Rendek (2008). Empirical evidence on Student-t log-returns of diversified world stock indices. *Journal of Statistical Theory and Practice* **2**(2), 233–251.

Platen, E. & R. Rendek (2012). Approximating the numéraire portfolio by naive diversification. *Journal of Asset Management* **13**(1), 34–50.

Revuz, D. & M. Yor (1999). *Continuous Martingales and Brownian Motion* (3rd ed.). Springer.

RiskMetrics (1996). *Technical Document* (4th ed.).

Ross, S. A. (1976). The arbitrage theory of capital asset pricing. *J. Economic Theory* **13**, 341–360.

Schroder, M. (1989). Computing the constant elasticity of variance option pricing formula. *J. Finance* **44**(1), 211–219.

Shiller, R. J. (2015). *Irrational Exuberance*. Princeton University Press, SP500 data: http://www.econ.yale.edu/ shiller/.

Wiggins, J. B. (1987). Option values under stochastic volatility. Theory and empirical estimates. *J. Financial Economics* **19**, 351–372.